Human N-Methyl-D-aspartate receptor antibodies alter memory and behavior in mice

Jesús Planagumà PhD[1,2*], Frank Leypoldt MD PhD[1,3*], Francesco Mannara BS[1,4*], Javier Gutiérrez-Cuesta PhD[4], Elena Martín-García PhD[4], Esther Aguilar BS[1], Maarten J. Titulaer MD PhD[5], Ankit Jain BS[6], Rita Balice-Gordon PhD[6], Melike Lakadamyali PhD[2], Francesc Graus MD[1,7], Rafael Maldonado PhD[4], and Josep Dalmau MD PhD[#1,8,9]

*contributed equally

[1]Institut d'Investigacions Biomèdiques August Pi i Sunyer (IDIBAPS), Hospital Clínic, Universitat de Barcelona, Barcelona, Spain

[2]ICFO-Institut de Ciències Fotòniques, Barcelona, Spain

[3]Department of Neurology and Institute of Clinical Chemistry, University Medical Center Schleswig-Holstein Campus Lübeck (Germany)

[4]Laboratori de Neurofarmacología, Facultat de Ciències de la Salut i de la Vida, Universitat Pompeu Fabra, Barcelona, Spain

[5]Department of Neurology, Erasmus Medical Center, Rotterdam, the Netherlands

[6]Department of Neuroscience, University of Pennsylvania, PA, USA

[7]Servei de Neurología, Hospital Clínic, Universitat de Barcelona, Barcelona, Spain

[8]Department of Neurology, University of Pennsylvania, Philadelphia, PA, USA

[9]Institució Catalana de Recerca i Estudis Avançats (ICREA), Barcelona, Spain

Running Title: Mouse model of antibody effects in anti-NMDA receptor encephalitis

Abstract word count: 200

Manuscript word count: 9988. It contains 2 tables and 8 figures.

Key words: Animal model, anti-NMDAR encephalitis, antibodies, passive transfer

Study supported by: This work was supported by the National Institutes of Health RO1NS077851 (JD), RO1MH094741 (R. B-G and JD), Fundació La Marató de TV3 (JD), Fondo de Investigaciones Sanitarias/Instituto Carlos III (FIS PI11/01780 JD), ErasmusMC fellowship (MT), and Forschungsförderungsfonds Hamburg-Eppendorf FL).

Conflicts of interest: Dr. Dalmau holds a patent for the use of NMDA receptor as autoantibody test. Dr. Dalmau has received a research grant from Euroimmun Inc

[#] Corresponding author: Josep Dalmau, MD, PhD, IDIBAPS-Hospital Clínic, Universitat de Barcelona, Department of Neurology, c/ Villarroel 170, Barcelona, 08036 (Spain)

Phone: +34 932 271 738, e-mail: jdalmau@clinic.ub.es

Abstract

Anti-N-Methyl-D-aspartate receptor (NMDAR) encephalitis causes severe neuropsychiatric symptoms with prominent memory and behavioral deficits. Patients' antibodies react with the N-terminal domain of GluN1 subunit of NMDAR causing in cultured neurons a selective and reversible internalization of cell-surface receptors. These effects and the clinical response to immunotherapy have suggested an antibody-mediated pathogenesis. Here we show that mice treated with continuous 14-day cerebroventricular infusion of patients' CSF, but not control CSF, developed progressive memory deficits, anhedonia, and depressive-like behaviors. Memory deficits gradually worsened until day 18 (4 days after the infusion stopped) and all symptoms resolved over the next week. Accompanying brain tissue studies showed progressive increase of brain-bound human antibodies, predominantly in the hippocampus (maximal on days 13-18), which after acid-extraction and characterization with GluN1-expressing HEK cells were confirmed to be against NMDAR. Confocal microscopy and immunoblot analysis of the hippocampus showed progressive decrease of clusters of total and synaptic NMDAR and total NMDAR protein concentration (maximal on day 18), without affecting PSD95, and minimally decreasing cell-surface AMPAR. These effects occurred in parallel with mice memory and other behavioral deficits and gradually improved after day 18, with accompanying decrease of brain-bound antibodies and recovery of NMDAR levels, confirming the antibody pathogenicity.

Introduction

Memory, learning, and behavior depend on the proper function of the excitatory glutamate NMDA receptors (NMDAR) and AMPA receptors (AMPAR) and underlying mechanisms of synaptic plasticity (1, 2). The critical role of NMDAR in these functions has been shown in animal models in which the NMDAR are altered genetically (3, 4) or pharmacologically (5, 6). In humans this evidence comes from more indirect observations such as studies investigating the effects of phencyclidine or ketamine (noncompetitive antagonists of NMDARs causing psychosis) (7, 8), and brain tissue studies of patients with schizophrenia or Alzheimer's disease in which several molecular pathways that modulate glutamate receptor trafficking or function are affected (9, 10). In 2007 we identified a novel disorder (anti-NMDAR encephalitis) that occurs with highly specific antibodies against extracellular epitopes located at the amino terminal domain of GluN1 subunit of the NMDAR (11, 12). The resulting syndrome resembles the spectrum of symptoms that occurs in genetic or pharmacologic models of NMDAR hypofunction, including memory loss and neuropsychiatric alterations ranging from psychosis to coma (13). The importance of this disease is emphasized by the fact that 40% of the patients are children and young adolescents, and currently it is considered the most frequent neuronal-antibody associated encephalitis (14, 15). Most patients have systemic and intrathecal synthesis of antibodies, the latter likely produced by plasma cells contained in brain inflammatory infiltrates demonstrated in autopsy studies (13, 16). These long-lived plasma cells and persistent antibody synthesis may explain the lengthy symptoms of most patients (average hospitalization ~3 months) (13). Yet, despite the severity and duration of the disease, 80% of the patients have complete or substantial recovery after immunotherapy (14).

Investigations on the potential pathogenic role of patients' antibodies using cultured neurons showed that the antibodies caused crosslinking and selective internalization of NMDARs that correlated with the antibody titers and these effects were reversible after removing the antibodies (17). In contrast to these robust effects on NMDARs, patients' antibodies did not alter the localization or expression of other synaptic proteins, number of synapses, dendritic spines, dendritic complexity, or cell survival. In parallel experiments, the density of NMDAR was also significantly reduced in the hippocampus of rats infused with patients' antibodies, a finding similar to that observed in the hippocampus of autopsied patients (17). Similar findings were reported by Mikasova and colleagues who showed that exposure of cultured neurons to patients' CSF blocked the induction of chemical long-term potentiation, as measured by a failure to increase synaptic content of surface AMPARs (18).

Overall, these studies established the mechanisms by which patients' antibodies caused a specific, titer-dependent, and reversible loss of NMDARs, but the effects on memory and behavior were not investigated. Based on these data and the experience with the human disease, we developed a murine model using a 14-day cerebroventricular infusion of patients' CSF. The aims were to determine if patients' antibodies altered memory and behavior, whether these effects correlated with brain antibody-binding and reduction of NMDAR levels, and whether these effects and associated symptoms recovered after stopping antibody infusion.

Results

Eighty-eight mice were included in the studies, 56 for cognitive and behavioral tests, and 32 for assessment of antibody binding to brain and the effects on total and synaptic NMDAR (Figure 1).

Cerebroventricular infusion of patients' CSF alters memory and behavior in mice

The most robust effect during the 14-day infusion of patients' CSF was on the novel object recognition test in both the open field and V-maze paradigms (Figure 2A,B). Compared with animals infused with control CSF, those infused with patients' CSF showed a progressive decrease of the object recognition index in both paradigms indicative of a memory deficit (19-21). The memory deficit became significant on day 10 and was maximal on day 18 (four days after the infusion of CSF had stopped). When examined on day 25, the object recognition index had normalized and was similar to that of animals treated with control CSF (Figure 2A,B). For all time-points, the total time spent exploring both objects (internal control) was similar in animals infused with control or patients' CSF (Table 1).

The preference to drink sweetened water (sucrose preference test) was used as a measure of anhedonic behavior. Mice infused with patients' CSF and tested during the infusion period (day 10) had less preference for sucrose compared with mice infused with control CSF (Figure 2C). In contrast, the same mice tested 10 days after the infusion of CSF had stopped (day 24) showed a preference for sucrose similar to that of the control mice. The total consumption of water with and without sucrose was similar in both groups (internal control, Table 1). In addition, two tests of depressive-like behavior were performed. The tail-suspension test, performed on day 12, showed that animals infused with patients' CSF had longer periods of immobility compared with those infused with control CSF (Figure 2D). In contrast, six days after the infusion of CSF had stopped (day 20), no differences were noted with the forced swimming test (examining immobility in inescapable situations; Figure 2E, Table 1). Overall, these

findings suggest that the infusion of NMDAR antibodies was associated with anhedonic and depressive-like behaviors.

In contrast to the prominent memory deficit, along with anhedonia and depressive behavior, no significant differences were noted in tests of anxiety (black and white test, elevated plus maze test), aggression (resident-intruder test) and locomotor activity (Figure 2F-I).

Patients' antibodies bind to NMDAR in mouse brain

Animals infused with patients' CSF, but not control CSF, had progressively increasing human IgG immunostaining (representing IgG bound to brain) that correlated with the duration of the infusion. The distribution of IgG immunostaining predominated in regions with high density of NMDAR, mainly the hippocampus (Figure 3A), highly resembling that obtained with brain sections directly incubated with patients' CSF or a monoclonal antibody against the GluN1 subunit of the NMDAR (13). Upon quantification of immunostaining, the maximal antibody binding was identified in mice sacrificed on day 18, which had received 14 days of CSF infusion, compared with mice sacrificed on days 5 or 13 (Figure 3B,C). In animals sacrificed on days 26 and 46 the presence of IgG immunostaining progressively decreased. In the cerebellum, the IgG immunostaining was sparse and not significantly different between animals infused with patients' CSF or control CSF (data not shown).

Studies with immunofluorescence and confocal microscopy showed that in animals infused with patients' CSF the presence of hippocampal IgG was visible as a punctate immunolabeling on the surface of neurons and neuronal processes in contrast to mice infused with control CSF where minor amounts of IgG reactivity without preference for neuronal structures were noted (Figure 4A-D). In addition, the amount of

human IgG bound to all selected regions of hippocampus was significantly higher than in the control group (Figure 4E).

To determine if the IgG immunostaining represented brain-bound NMDAR antibodies, IgG was extracted from several brain regions and examined for reactivity with HEK cells expressing GluN1. These studies showed that the IgG extracted from hippocampus of mice infused with patients' CSF reacted specifically with GluN1 (Figure 5A). The NMDAR antibody concentration in the extracts correlated with the duration of infusion of CSF; it increased until day 13, reached the maximal concentration on days 13-18, and decreased afterwards (Figure 5A,C). NMDAR antibodies were also detected in IgG extracts from other brain regions (frontal cortex, cerebellum) but at lower concentration to that obtained in fractions extracted from hippocampus (Figure 5D). Demonstration that the extracted antibodies were specifically bound to the NMDAR was provided by the lack of GluN1 reactivity in the pre-extraction fractions (Figure 5B,E). Parallel studies with tissue from animals infused with control CSF did not show NMDAR antibodies (data not shown).

Patients' antibodies cause a decrease of the density of NMDAR clusters and total NMDAR protein in mice hippocampus

We previously reported that patients' CSF antibodies caused a decrease of the density of cell surface and synaptic NMDAR clusters as well as total NMDAR protein in cultured hippocampal neurons, and similar effects were observed after injection of CSF antibodies into rat hippocampus (17). These effects were specific for NMDAR without affecting PSD95 and correlated with the titer of patients' antibodies. In the current study, the experiments on the effect of patients' antibodies were focused on the hippocampus, which was the region with maximal concentration of NMDAR-bound

antibodies. Compared with animals infused with control CSF those infused with patients CSF had on days 13 and 18 a significant decrease of the density of total and synaptic hippocampal NMDAR clusters followed by a gradual recovery after day 18 (pooled analysis of CA1, CA3 and DG, Figure 6A-D). No significant differences in between hippocampal subregions (CA1, CA3, DG) were observed (not shown). In contrast, the effect of patients' antibodies on the density of PSD95 did not show significant changes (Figure 6E). A small reduction of total AMPAR clusters was noted on day 18 (other time points not examined; Figure 6F).

Immunoblot analysis of total protein extracted from hippocampus isolated from tissue sections showed that on day 13 and 18, mice infused with patients' CSF had a significant decrease of total NMDAR protein concentration compared with mice infused with control CSF (Figure 7A,B). The magnitude of this effect was greater in animals with higher concentration of IgG bound to hippocampus (Figure 7C). Parallel studies examining the effect on the total protein concentrations of PSD95 (Figure 7A,D) and AMPAR (Figure 7E) demonstrated no significant differences between mice infused with patients' CSF or control CSF.

In cerebellum, no significant effects on the cluster density or total protein concentration of NMDAR, PSD95 and AMPAR were noted animals infused with patients' CSF compared to those infused with control CSF (data not shown).

Immunohistochemical studies for neuronal apoptosis (TUNEL/cleaved caspase-3), T- or B-cell infiltrates, and deposits of complement in CA1, CA3, and DG in animals infused with patients' or control CSF, examined on day 18, showed no evidence of apoptosis, inflammatory infiltrates or deposits of complement (Figure 8).

Discussion

We report that passive transfer of NMDAR antibodies by continuous ventricular infusion of CSF from patients with anti-NMDAR encephalitis causes memory and behavioral deficits in mice, and that the effects are likely mediated by the binding of antibodies to NMDAR resulting in a specific decrease of the density of these receptors. Data from early reports showing that despite the severity and duration of symptoms most patients with anti-NMDAR encephalitis respond to immunotherapy, and findings at the cellular level demonstrating that patients' antibodies cause a titer-dependent decrease of synaptic NMDAR receptors, fulfilled most of the Witebsky's criteria for an antibody-mediated disorder (22), but the transfer of symptoms to animals was pending. In the current study, four sets of experiments satisfy this postulate, 1) the development of symptoms in animals infused with patients' CSF, but not control CSF, 2) the demonstration that the infused antibodies reacted predominantly with brain regions with high density of NMDAR (e.g., hippocampus) and specifically recognized these receptors, 3) the identification of a selective decrease of the density of total and synaptic NMDAR clusters and total NMDAR protein concentration without affecting PSD95, and that these effects correlated with the concentration of brain-bound antibodies, and 4) the correlation noted between the intensity of the above-mentioned findings and the time-course of patients' antibody infusion, and the reversibility of symptoms and restoration of NMDAR levels after stopping the infusion.

Approximately 75% of patients with anti-NMDAR encephalitis present with mood, behavioral, and psychiatric alterations ranging from depression or agitation to psychosis, and often followed by stereotyped movements, seizures, or decreased level of consciousness (14). Regardless of the presentation, most patients develop severe

problems forming new memories and amnesia of the disease. In addition, close examination during the phase of recovery sometimes shows impairment in the visual recognition of objects or faces (e.g., physicians, nurses) (23). Owing to the wide range of symptoms of the disease and lack of previous studies examining the distribution of NMDAR antibody binding when these antibodies are infused intraventricularly, we used standardized memory and behavioral tests. The most notable effects were observed in the tests of memory (novel object recognition) using different groups of animals in two different paradigms (open field and V-maze). While the first depends predominantly on normal hippocampal function, the second is dependent of perirhinal-hippocampal structures (24). Compared with animals infused with control CSF, those infused with patients' CSF developed progressive memory deficits which were maximal on days 13-18 when the highest concentration of brain-bound NMDAR antibodies and lowest density of NMDAR occurred. Other paradigms affected were related to depressive-like behaviors (tail suspension test) and anhedonic-depressive behaviors (sucrose preference test). We did not find significant abnormalities in the tests of aggression and anxiety, which are often present in the human disease, or in locomotor activity (an expected finding given that motor deficits or paralysis rarely occurs in patients).

The high levels of brain-bound NMDAR antibodies between days 13-18 suggests that after stopping the infusion of patients' CSF on day 14, the NMDAR antibodies continued being distributed from mice CSF to parenchyma resulting in a progressive decrease of NMDAR and worsening memory and behavioral deficits for at least 4 days before recovery begins. Although the hippocampus was the region with the highest concentration of brain-bound NMDAR antibodies, these antibodies were also extracted from cerebral cortex and cerebellum though at lower levels. The higher

concentration of antibodies and predominant decrease of NMDAR in hippocampus are consistent with the predominant binding of human antibodies to hippocampus when sections of rodent brain are directly incubated with patients' antibodies (11). Additionally, the infusion of human CSF antibodies through the ventricles might have also contributed to the predominant binding in the hippocampus which is closely located to a region with impaired BBB function due to the presence of the cannula. The correlation between the concentration of brain-bound antibodies and selective reduction of NMDAR clusters and protein concentration was similar to that previously reported using cultured rat hippocampal neurons treated with CSF from patients with different titers of antibodies (17, 18). Moreover, autopsies of patients with anti-NMDAR encephalitis showed that the hippocampal regions with highest concentration of brain-bound antibodies were also the areas with lower expression of NMDAR.(11) While previous studies examining the effects of patients' antibodies in cultured neurons showed that the levels of AMPAR were not affected (17), the current study with brain of infused mice shows a small, but significant reduction of total AMPAR clusters. This finding would be in line with the observation of Mikasova and colleagues that neurons exposed to patients' NMDAR antibodies failed to show an increase in cell surface AMPAR after induction of chemical long-term potentiation (18). Moreover, analysis of the acute metabolic effects of patients' antibodies after injection to rat brain showed impairment of NMDA and AMPA-mediated synaptic function (25).

This study has limitations related to the complexity of the disease, the approach used, and the strain of mice. For example, different from other models of antibody-mediated disorders where the target antigen is in the CNS and the effects are focal deficits associated with visible tissue changes (e.g., demyelination in neuromyelitis optica) (26), anti-NMDAR encephalitis results in a broader spectrum of symptoms

where memory and behavior are affected early, and structural alterations are not visible unless the NMDAR clusters or protein concentration are measured. It is not surprising that in the current model the full spectrum of symptoms, such as seizures, dyskinesias, or coma, did not occur. Studies with NMDAR antagonists have shown that the progression of symptoms (from memory and behavioral problems to unresponsiveness with catatonic features and coma) correlated with the intensity of the decrease of receptor function (27). It is likely that higher titer or prolonged infusion of patients' antibodies would result in additional symptoms. This is supported by the current model in which the time course of symptom development, brain-bound antibody concentration, and decrease of NMDAR correlated well with each other. Moreover, the strain of mice used (C57BL6/J) is optimal for some behavioral studies but particularly resistant to seizures (28).

The current findings provide robust evidence that antibodies from patients with anti-NMDAR encephalitis change memory and behavior through alteration of cell surface and synaptic NMDAR. This approach can now be adapted to 1) model other aspects of the disease by changing the duration and dosing of antibody infusion, or strain of mice, 2) investigate other disorders of memory and behavior that occur in association with antibodies against other cell surface or synaptic proteins, such as AMPAR or GABAR (29, 30), and 3) determine whether compounds such as Ephrin-B2 ligand, which binds to Eprin-B2 receptors and has been shown to prevent the destabilizing NMDAR crosslinking effects of patients' antibodies (18), improve or alter the course of the disease.

Methods

Animals

Male C57BL6/J mice (Charles River), 8-10 weeks old (25-30 g) were housed in cages of 5 until one week before surgery, when they were housed individually. The room was maintained at a controlled temperature (21±1ºC) and humidity (55±10%); food and water were available *ad libitum*, with illumination at 12 hour cycles. All experiments were performed during the light phase, and animals were habituated to the experimental room for 1 week before starting the tests. All procedures were conducted in accordance with the standard ethical guidelines (European Communities Directive 86/609/EU) and approved by the local ethical committees: Comitè Ètic d'Experimentació Animal, Institut Municipal d'Assistència Sanitària, Universitat Pompeu Fabra, and Instituional Animal Care and Use Committee (IACUC, University of Pennsylvania).

Patients´ CSF samples

To develop this model we took in consideration that most patients with anti-NMDAR encephalitis have intrathecal synthesis of antibodies leading to high CSF antibody titer (13, 31). While patients might also have serum antibodies due to systemic synthesis, the CSF contains orders of magnitude less amounts of other proteins making it an ideal source of antibodies. The CSF were individually pre-screened using two previously reported assays, 1) Immunohistochemistry with rodent brain adapted to determine antibodies against cell surface and synaptic proteins (it provides a highly characteristic pattern of NMDAR staining and rules out the presence of other antibodies) (13), and 2) a cell-based assay with human epithelial kidney (HEK) 293 cells expressing the GluN1 subunit of the NMDAR (it confirms the antibody specificity) (13, 32). Dialyzed CSF from 25 patients with high titer NMDAR antibodies (all >1:320) were pooled and used for cerebroventricular infusion. CSF samples from 11 patients with normal pressure hydrocephalus and 14 non-inflammatory CNS disorders were similarly pre-screened

and used as controls. Studies were approved by the institutional review board of Hospital Clínic and Institut d'Investigacions Biomèdiques August Pi i Sunyer (IDIBAPS), Universitat de Barcelona.

Surgery, placement of ventricular catheters and osmotic pumps

The cerebroventricular infusion of CSF was performed using osmotic pumps (model 1002, Alzet, Cupertino, CA) with the following characteristics: volume 100 µl, flow rate 0.25 µl/hr, an d duration 14 days. Twenty-four hours before surgery, two osmotic pumps per animal were each loaded with 100 µl of patients' or control CSF. The pumps were then connected to a 0.28 mm IM (internal diameter) polyethylene tube (C314CT, PlasticsOne) and left overnight in sterile phosphate buffered saline (PBS) at 37°C. The next day, mice were deeply anesthetized by intraperitoneal injection of a mixture of ketamine (100 mg per kg) and xylazine (10 mg per kg) along with subcutaneous administration of the analgesic meloxicam (1mg per kg). Mice were then placed in a stereotaxic frame, and a bilateral catheter (PlasticsOne, model 3280PD-2.0/SP) was inserted into the ventricles (0.02 mm anterior and 1.00 mm lateral from bregma, depth 0.22 mm) and secured with dental cement. Each arm of the catheter was connected to one osmotic pump, which were subcutaneously implanted on the back of the mice. Appropriate ventricular placement of the catheters was assessed in randomly selected mice injecting methylene blue through the catheters (Figure 1B-D).

Cognitive tasks

All behavioral tasks were performed by researchers blinded to experimental conditions using standardized tests reported by us (19, 21, 33-40) and others (20, 41-46) and following the schedule summarized in Figure 1A. The tasks were aimed to assess

memory (novel object recognition in open field and V-maze), anhedonic behaviors (sucrose preference test), depressive-like behaviors (tail suspension, and forced swimming tests), anxiety (black and white and elevated plus maze tests), aggressiveness (resident-intruder test) and locomotor activity (horizontal and vertical activity assessment).

Novel object recognition (NOR) test: This test was performed in two paradigms, open field (45x45x40 cm, Panlab, Spain) and in V-maze (40 cm per side, Panlab, Spain) using two different groups of animals, as reported by us and others (19-21). On day 1 (same day of osmotic pump implantation, before surgery) mice were habituated for 30 minutes in the open field arena, or 9 minutes in the V-maze. On days 3, 10, 18 and 25, mice were put back into the open field arena or into the V-maze for 9 minutes; two identical objects were presented, and the time the mice spent exploring each object was recorded. After a retention phase of 3 hours, the mice were placed for another 9 minutes into the open field arena or into the V-maze; in each paradigm one of the familiar objects was replaced with a novel object and the total time spent exploring each object (novel and familiar) was registered. During the test phase of the open field paradigm, the objects were positioned in the opposite corners of those used in the training phase and the novel object was presented in 50% of trials on the right and in 50% of trials on the left side. Object exploration was defined as the orientation of the nose to the object at a distance of less than 2 cm. A discrimination index was calculated as the difference of the time spent exploring the novel and the time spent exploring the familiar object divided by the total time exploring both objects. A higher discrimination index is considered to reflect greater memory retention for the familiar object (21, 47).

Sucrose preference test: This test was performed on days 10 and 24 after surgery, as previously reported (35, 42). During the 4 days preceding surgery, two bottles of water, one with 2% sucrose and the other without, were placed in the cage. Every day the position of the bottles was exchanged, and the consumption from each bottle measured. On the day of the test, the two bottles were placed again in the cage and the consumption from each recorded after a 24h interval. The preference for sucrose was calculated as the relative amount of water with sucrose versus total liquid (water with and without sucrose) consumed by the mice.

Tail suspension test (TST): This test was performed on day 12 after surgery, as previously reported (33, 41). Mice were suspended 50 cm above a solid surface by the use of adhesive tape applied to the tail (3/4 of the distance from the base of mouse tail). During a six minutes interval, the total time of immobility was recorded. Long periods of immobility are characteristic of a depressive-like state; an alternative test is the forced swimming test, which was also applied at a different time point (see below).

Forced swimming test (FST): This test was performed on day 20 after surgery, as previously reported (38, 46). The mouse was placed in a plastic cylinder containing warm water (27-28 °C), deep enough to prevent touching the bottom of the cylinder and forcing the mouse to swim. The trial lasted 6 minutes and the total time of immobility after minute 2:00 was recorded. Time of immobility was defined as the time that the animal stopped swimming and only used minimal movements to keep the head above the water.

Black and white test: This test was performed on day 6 after surgery, as reported (36, 44). It measures the conflict between the natural tendency of rodents to explore new environments and the tendency to avoid brightly illuminated areas. The box consisted of two compartments (20 cm wide × 20 cm long × 30 cm high) connected by a 6 cm wide by 6 cm high tunnel. A compartment was painted black and maintained at 10 lux, while the other compartment was painted white, brightly illuminated (500 lux), and subdivided in 3 sections (distal, medial and proximal), based on the distance from the tunnel. The floor of both compartments was subdivided into squares (5x5 cm) to measure the locomotor activity. At the start of the session, mice were placed in the black compartment, head facing a corner. The latency of first entry into the white compartment and section reached in each entry, together with time spent, squares crossed, and number of entries into both compartments were recorded and used to evaluate anxiety.

Elevated plus maze test: This test was performed on day 14 after surgery, as reported (39, 48). The test is based on the same principle as the black and white test, and measures the conflict between the natural tendency of mice to avoid an illuminated and elevated surface, and the natural tendency to explore new environments. It consisted of a plastic black cross with arms 40 cm long and 6 cm wide placed 50 cm above the floor. Two opposite arms were surrounded by walls (15 cm high, closed arms, 10 lux), while the two other arms were devoid of such walls (open arms, 200 lux). The four arms were connected by a central platform. At the start of the session, the mouse was placed at the end of a closed arm facing the wall. During the 5-minute trial, the number of entries and the time spent in each arm were recorded. Anxiety was assessed as both the time spent avoiding the open arms and the number of entries into them.

Resident-intruder test: This test, performed on days 3, 10, 18 and 25 after surgery, evaluates aggressive behavior in rodents, as reported (37, 45). Resident mice were housed individually for at least 10 days before the test. Intruder animals of similar age and weight were housed five per cage. Each session consisted of putting together resident and intruder mice for a period of 4 minutes, measuring the latency of the first aggressive event and frequency of events.

Locomotor activity: This test was performed on days 3, 10, 18 and 25 after surgery. Animals were assessed in locomotor activity boxes (9×20×11 cm; Imetronic, Passac, France), equipped with 2 rows of photocell detectors, and placed in a low-luminosity environment (20–25 lux), as previously described (34, 43). The mouse locomotor activity was recorded for 10 minutes as horizontal activity and vertical activity.

Brain tissue processing

To determine the effects of patients' antibodies on mouse brain, animals were sacrificed at the indicated time points (Figure 1A, Days 0, 5, 13, 18, 26 and 46) with CO_2. Brains were harvested, hemispheres sagittally split, and transferred to ice-cold PBS. Half of the brain was fixed by immersion in 4% paraformaldehyde (PFA) for 1 hour at 4°C, cryoprotected with 40% sucrose for 48 hours at 4°C, embedded with freezing media (Tissue-Tek OCT compound, Sakura Finetek, Leiden, The Netherlands), snap frozen with isopentane chilled with liquid nitrogen, and kept at -80°C until sectioning. The other half brain was used for dissection of hippocampus and cerebellum for IgG and protein extraction (see below).

Immunohistochemistry and quantitative peroxidase staining

For determination of antibodies bound to brain using immunoperoxidase staining, 7 µm-thick tissue sections were sequentially incubated with 0.25% H_2O_2 for 10 minutes at 4°C, 5% goat serum for 15 minutes at room temperature (RT), biotinylated goat anti-human IgG (1:2000, Vector labs, Burlingame, CA, USA) overnight at 4°C, and the reactivity developed using avidin-biotin-peroxidase (ABC Elite, Vector) and diaminobenzidine (DAB). Sections were mildly counterstained with hematoxylin, mounted, and results photographed (1.5x for full brain and 4x for hippocampus) under a Leica DMD108 microscope (Mannheim, Germany). Images were prepared creating a mask for DAB color, converting the mask to grey scale intensities, and inverting the pixels using Adobe Photoshop CS6 package. Hippocampal and cerebellar regions were manually outlined; intensity and area were quantified in two serial sections using the public domain Fiji ImageJ software (http://fiji.sc/Fiji). Values were divided by area and normalized to the group with the highest mean (defined as 100%, patients' CSF treated animals sacrificed at day 18).

Immunofluorescence and confocal microscopy with brain tissue

For determination of antibodies bound to brain using immunofluorescence, 5 µm-thick tissue sections were blocked with 5% goat serum and 1% bovine serum albumin (BSA) for 60 minutes at RT, and incubated overnight at 4°C with Alexa Fluor 488 goat anti-human IgG (A11013, diluted 1:1000, Molecular Probes/Life Technologies, Carlsbad, CA, USA). Slides were then mounted with anti-fading agent ProlonGold (P36930, Molecular Probes/Life Technologies) and results scanned under a LSM710 Zeiss confocal microscope. Sections from all animals were analyzed in parallel. Quantification of fluorescent intensity in areas of CA1, CA3 and DG was done using

Fiji ImageJ software. Background was subtracted and intensity divided by area. Mean intensity of IgG immunostaining in animals treated with patients' CSF and sacrificed at day 18 was defined as 100%.

The effect of patients' antibodies on synaptic NMDAR clusters was determined comparing the density and co-localization of NMDAR clusters with PSD95. For this, non-permeabilized 5 μm-thick sections were blocked with 5% goat serum and 1% BSA as above, incubated with human CSF antibodies for 2 hours at RT, washed with PBS, permeabilized with Triton 0.3% for 10 minutes at RT, and incubated with rabbit polyclonal antibody against PSD95 (diluted 1:250, Clone 18258 Abcam, Cambridge, UK) overnight at 4°C. Next day, the slides were washed and incubated with the corresponding secondary antibodies, Alexa Fluor 594 goat anti-human IgG and Alexa Fluor 488 goat anti-rabbit IgG (A-11014, A-11008, both diluted 1:1000, Molecular Probes/Life Technologies) for 1 hour at RT. Slides were mounted as above and results scanned with a confocal microscope (Zeiss LSM710) with EC-Plan NEOFLUAR CS 100x/1.3 NA Oil objective. Standardized z-stacks including 50 optical images were acquired from five different, equally spaced areas of CA1, CA3, and dentate gyrus (DG) of hippocampus using sequential scanning, 1024×1024 lateral resolution, and Nyquist optimized z sampling frequency. Images were deconvolved with 20 iterations using theoretical point spread functions and maximum likelihood estimation algorithms of Huygens Essential software (Scientific Volume Imaging BV, Hilversum, the Netherlands). For cluster density analysis a spot detection algorithm from Imaris suite 7.6.4 (Bitplane, Zurich, Switzerland) was used based on automatic segmentation of the images to spots (49). Density of clusters was expressed as spots/μm3. Three-dimensional colocalization of clusters (e.g. NMDAR and PSD95) was done using a spot-colocalization algorithm implemented in Imaris suite 7.6.4. Synaptic localization

was defined as colocalization of NMDAR or AMPAR with postsynaptic PSD95. Synaptic cluster density was expressed as colocalized spots/μm3. For each animal, five identical image stacks in each hippocampal area (CA1, CA2 and DG) were acquired and the mean densities calculated for total and synaptic NMDAR and AMPAR. Densities were normalized to the mean density of control CSF treated animals (100%). Antibodies used were guinea pig GluA1 antibody (1:100, clone AGP-009, Alomone, Jerusalem, Israel), and as secondary antibody Alexa Fluor 594 goat anti-guinea pig IgG (A11076, 1:1000, Molecular Probes/Life Technologies).

The presence of apoptosis, cellular infiltrates, and complement was assessed in the hippocampal region (CA3) that showed the maximal effects of patients' antibodies in mice sacrificed on day 18 and corresponding controls. Apoptosis was determined by standard terminal deoxynucleotidyl transferase mediated biotinylated UTP nick end labeling (TUNEL) using the TACS 2TdT-Fluor in situ apoptosis detection kit (Trevigen, Gaithersburg, MD, USA), and immunolabeling of cleaved caspase 3 (1:200, #9661 Cell Signalling, Technologies, Danvers, MA, USA) using a goat anti rabbit – Alexa 488 as secondary antibody (1:1000 Molecular Probes/Life Technologies). The presence of complement was assessed using rabbit anti-mouse C5b-9 (1:500, Abcam) and Alexa Fluor 488 goat anti-rabbit IgG (1:500, #A11008, Molecular Probes/Life Technologies). Immunolabeling for B- and T lymphocytes was done using rabbit anti-mouse CD3 (1:1000, #ab16669 Abcam) followed by secondary antibody goat anti-rabbit Alexa Fluor 488 (1:1000, Molecular Probes/Life Technologies), and rat anti-CD45R (1/10000, #ab64100) followed by goat anti-rat Alexa Fluor 594 (1/1000, #A-11007 Molecular Probes/Life Technologies). Slides were mounted and results scanned with a confocal microscope (Zeiss LSM710).

Extraction of human IgG bound to mice brain

Under a dissection microscope (Zeiss stereomicroscope, Stemi 2000), the hippocampus and cerebellum were isolated, weighed, snap frozen, and stored at -80°C until further analyzed. 10 mg tissue was homogenized in 0.5 ml ice-cold PBS with protease inhibitors (Sigma-Aldrich, St. Louis, MO, USA) and centrifuged at 16.000g for 5 minutes. All steps were performed at 4°C. Washing was repeated four times to remove unbound IgG. The last washing step was done in 100µl and the supernatant saved as pre-extraction fraction. To extract the specifically bound antibodies, the pellet was solubilized in 86µl 0.1M Na-citrate buffer pH2.7, incubated for 5 minutes, centrifuged at 16.000g for 5 minutes, and the supernatant neutralized with 14µl 1.5M Tris pH8.8, and used in a cell-based assay for determination of GluN1 (NMDAR) antibodies (see below).

Immunofluorescence with HEK293 cells expressing GluN1

The presence of GluN1 antibodies in IgG extracts from brain was determined using a cell-based assay with HEK293-cells transfected with GluN1, as reported (13). In brief, cells were grown for 24 hours after transfection before assessment. Transfected cells were then fixed with 4% PFA for 10 minutes at RT, permeabilized with 0.3% Triton X-100 (Sigma-Aldrich) for 5 minutes at RT, blocked with 1% BSA for 1.5 hours, and incubated with undiluted acid-extracted IgG or pre-extraction fraction from brain of infused mice, at 4°C overnight. The next day, cells were washed and incubated with a mouse monoclonal antibody against a non-competing GluN1 epitope located at amino acid 660-811 (1:20.000; clone MAB363, Millipore) for 1 hour at RT, followed by the corresponding secondary antibodies, Alexa Fluor 488 goat anti-human IgG and Alexa Fluor 594 goat anti-mouse IgG (A11013, A11032, both diluted 1:1000, Molecular

Probes/Life Technologies) for 1 hour at RT. The titer of positive samples was calculated by serial dilutions of the extracted IgG until the reactivity with HEK293 cells expressing GluN1 was no longer visible. Results were photographed under a fluorescence microscope using Zeiss Axiovision software.

Immunoblot analyses

Total protein from hippocampus and cerebellum was obtained by dissecting these regions from 20 µm-thick PFA-fixed sagittal mouse brain sections on glass slides at 4°C under a dissection microscope (Zeiss stereomicroscope, Stemi 2000). Two consecutive sections of isolated hippocampus or cerebellum were then transferred to an Eppendorf tube in PBS supplemented with protease inhibitors. Loading buffer (RotiLoad, Roth, Karlsruhe, Germany) was added, the solubilized tissue boiled for 5 minutes, and the proteins separated in a 10% SDS gel electrophoresis with semi-dry blotting on PVDF membranes. Membranes were blocked in 5% non-fat skim milk (Sigma-Aldrich) and incubated overnight at 4°C with the following polyclonal rabbit antibodies: GluN1 (1:1000, Sigma-Aldrich), GluR2/3 (1:1000, Abcam), and PSD95 (1:1000, Synaptic Systems, Goettingen, Germany), or a monoclonal mouse anti-β-actin (1:20.000, Sigma-Aldrich). Membranes were incubated with secondary antibodies for 1 hour at RT (anti-rabbit-IgG-HRP 1:1000, anti-mouse-IgG-HRP 1:10.000) and analyzed by enhanced chemiluminescence (all Amersham-GE Healthcare, Pittsburgh, PA, USA) on a LAS4000 (GE Healthcare, Pittsburgh, PA, USA). All analyzed films were in the linear range of exposure, digitally scanned, and signals quantified using Fiji ImageJ software. Proteins from hippocampus or cerebellum of mice infused with patients or control CSF sacrificed at the same time points were analyzed in the same membrane; all studies were done in duplicate. The signal intensity of each antigen was normalized to that of actin in

the same lane. The mean intensity of signal in control CSF treated animals was defined as 100% and all other intensities expressed in percent relative to this value.

Statistics

Behavioral tests were analyzed using repeated measures two-way ANOVA for tests with multiple time points ((novel object recognition, sucrose preference test, resident-intruder test, locomotor activity), independent sample-t tests for tests with single time-points (forced swimming test, black and white test, elevated plus maze test) or by Mann Whitney U for skewed distributions (tail suspension test). Non-normally distributed parameters were log-transformed (black and white test, elevated plus maze test). Significance of NMDAR antibody titer in acid-extracted IgG fractions was calculated using the Kruskal-Wallis test and Dunn's post-hoc test compared to titers at day 46. Human IgG intensity, confocal cluster density and immunoblot data (NR1/PSD95) from different time points or regions were analyzed using two-way ANOVA with Sidak-Holm post-hoc testing to calculate multiplicity-adjusted p-values. Confocal cluster density in the different hippocampal subregions (CA1, CA3, DG) were not significantly different and were analyzed pooled. For confocal AMPAR density measured at single time points, independent sample-t tests were used. Human IgG intensity in immunohistochemistry was log-transformed because of non-normality. A p-value of < 0.05 was considered significant, in post-hoc testing after correction for multiple testing (Sidak-Holm). In the 2 way ANOVA the cut-off for interaction between 2 factors was set at 0.1; if the p-value for interaction was < 0.10, the effects of treatment were considered for the separate time points (post-hoc analysis). All tests were done using GraphPad Prism (Version 6, La Jolla, CA, USA).

Acknowledgements

We thank Anna Planas and Vanessa Brait for providing stroke brain tissue.

Figures

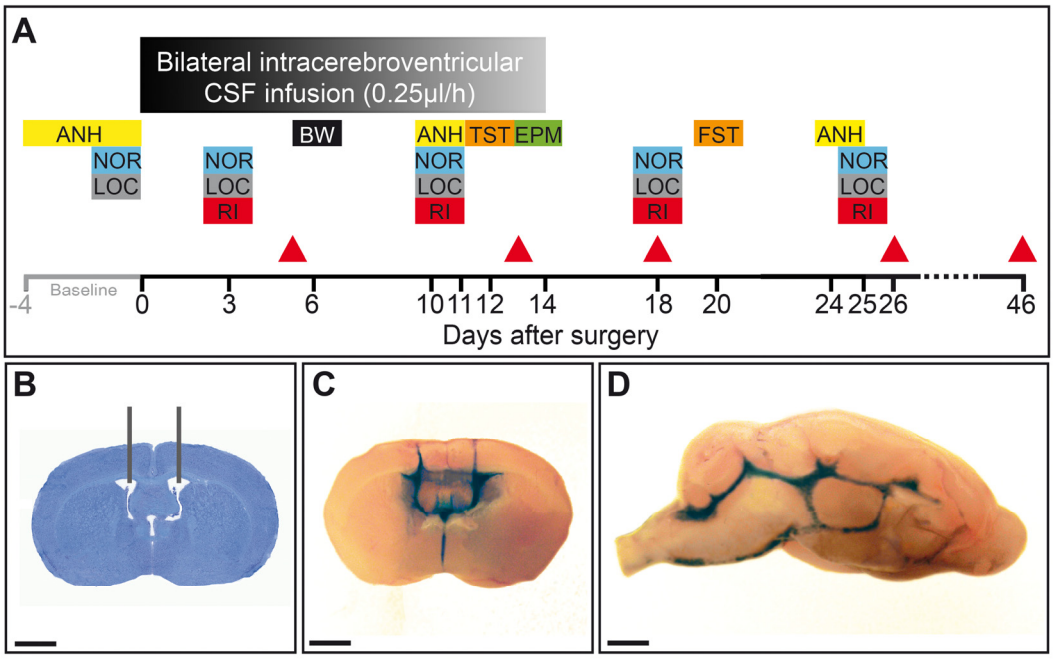

Figure 1: Experimental design and placement of ventricular catheters
(A) Schedule of cognitive testing and animal sacrifice. At day 0, catheters and osmotic pumps were placed and bilateral ventricular infusion of patients' or control CSF started. Infusion lasted for 14 days. Memory (novel object recognition [NOR]), anhedonia (sucrose preference test [ANH]), depressive-like behavior (tail suspension test [TST] and forced swimming test [FST]), anxiety (black and white test [BW] and elevated plus maze test [EPM]), aggressiveness (resident intruder test [RI]) and locomotor activity (LOC) were assessed blinded to treatment at the indicated days. The NOR was assessed in open field and V-maze paradigms in two different cohorts of mice. Animals were habituated for 1 to 4 days before surgery (baseline) to NOR, ANH, and LOC. Red arrowheads indicate the days of sacrifice for studies of effects of antibodies in brain.
(B) Representative coronal mouse brain section with catheter placement.
(C, D) Sagittal and coronal mouse brain sections demonstrating cerebroventricular diffusion of methylene blue after ventricular infusion. Scale bars=2 mm.

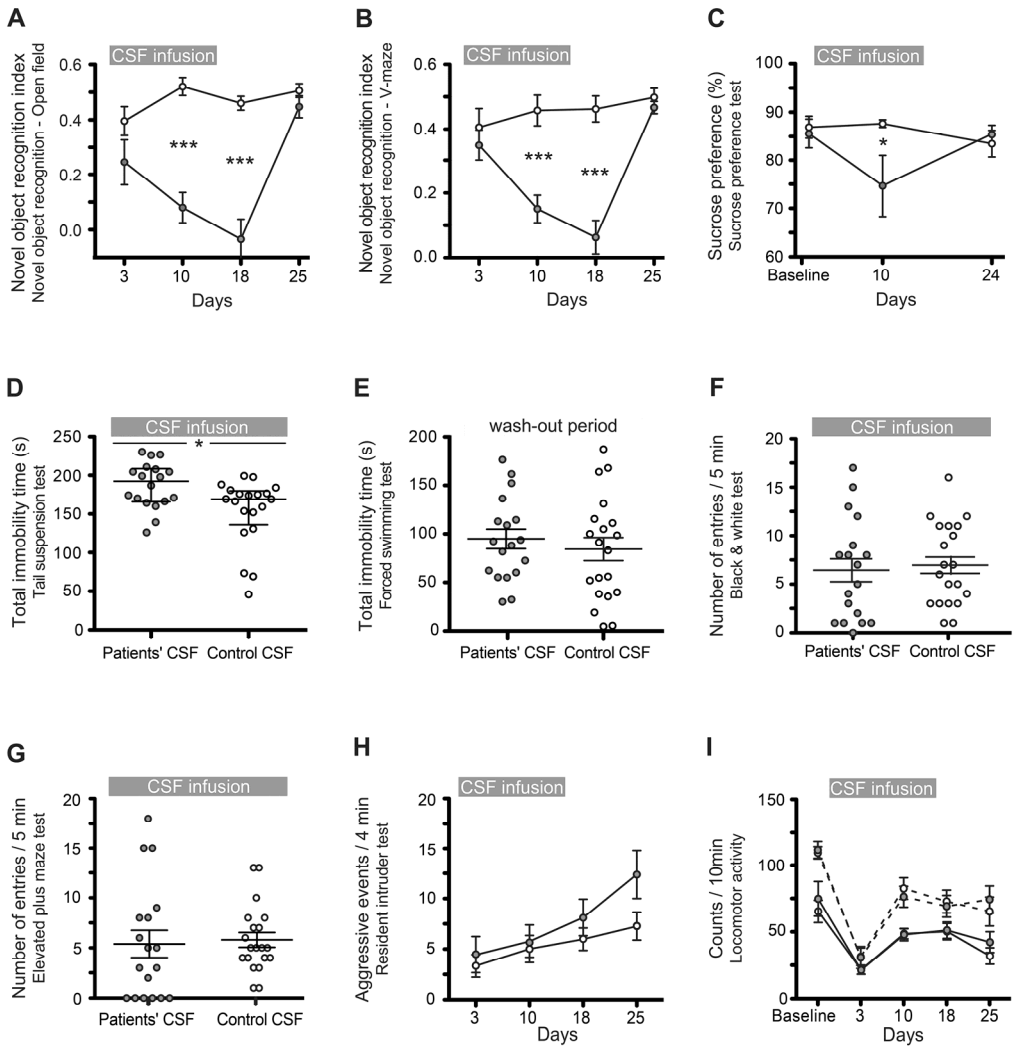

Figure 2: Infusion of CSF from patients with NMDAR antibodies causes deficits in memory, anhedonia, and depressive-like behavior

(A,B) Novel object recognition (NOR) index in open field (**A**) or V-maze paradigms (**B**) in animals treated with patients' CSF (grey circles) or control CSF (white circles) A high index indicates better object recognition memory. **(C)** Preference for sucrose-containing water in animals infused with patients CSF (grey) or control CSF (white). Lower percentages indicate anhedonia. **(D,E)** Total time of immobility in tail-suspension test during the infusion period (**D**, day 12), and in forced swimming test after the infusion period (**E**, day 20). **(F, G)** Number of entries into bright/open compartments during a five minute period in a standard black & white (**F,** day 6) or elevated plus maze test (**G,** day 14) in both treatment groups. (**H**) Number of aggressive events over a four minute period in a resident intruder paradigm in both treatment groups. (**I**) Horizontal (solid lines) and vertical (dashed lines) movement count over a ten minute period in both treatment groups. Data are presented as mean ± s.e.m (median ± IQR in **D).** Number of animals: Patients' CSF n=18 (open field NOR n=8), control CSF n=20 (open field NOR n=10). Significance of treatment effect was assessed by two-way ANOVA with an α-error of 0.05 and post-hoc testing with Sidak-Holm adjustment (asterisks), unpaired t-test or Mann-Whitney U test when appropriate.
* P<0.05, ** P<0.01, *** P<0.001. See Table 1 for detailed statistics.

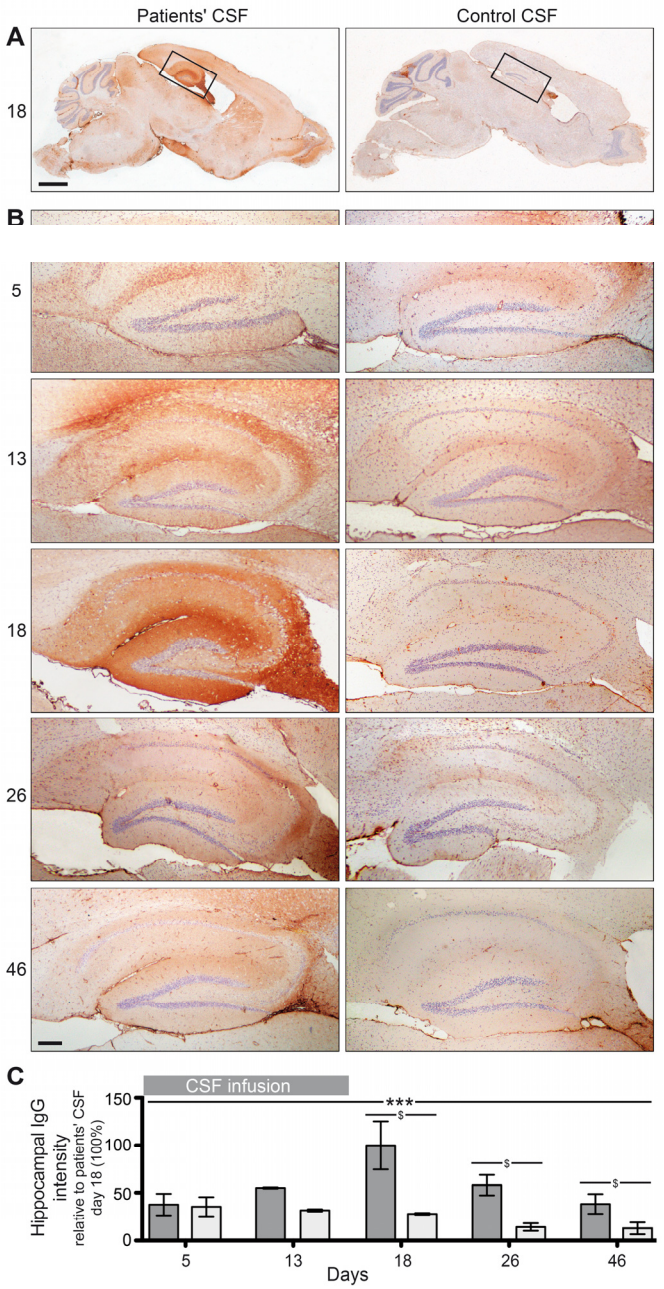

Figure 3: Animals infused with patient's CSF have a progressive increase of human IgG bound to hippocampus.

(A, B) Immunostaining of human IgG in sagittal brain sections (**A**) and hippocampus (**B**) of representative animals infused with patients' CSF (left panels) and control CSF (right panels), sacrificed at the indicated experimental days. In animals infused with patients' CSF there is a gradual increase of IgG immunostaining until day 18, followed by decrease of immunostaining. Scale bar in **A**=2 mm; scale bar in **B**=200 µm.

(C) Quantification of intensity of human IgG immunolabeling in hippocampus of mice infused with patients' CSF (grey columns) and control CSF (white columns) sacrificed at the indicated time points. Mean intensity of IgG immunostaining in the group with the highest value (animals treated with patients' CSF and sacrificed at day 18) was defined as 100%. Data are presented as mean ± s.e.m. Number of animals: treated with patients' CSF, sacrificed on day 5 n=3, day 13 n=4, day 18 n=4, day 26 n=4, and day 46 n=3; treated with control CSF, sacrificed on day 5 n=3, day 13 n=3, day 18 n=3, day 26 n=2, day 46 n=3. Significance of treatment effect was assessed by two-way ANOVA on log-transformed data with an α-error of 0.05 (asterisks) and post-hoc testing with Sidak-Holm adjustment ($). $ $P<0.05$, *** $P<0.001$. See Table 2 for detailed statistics.

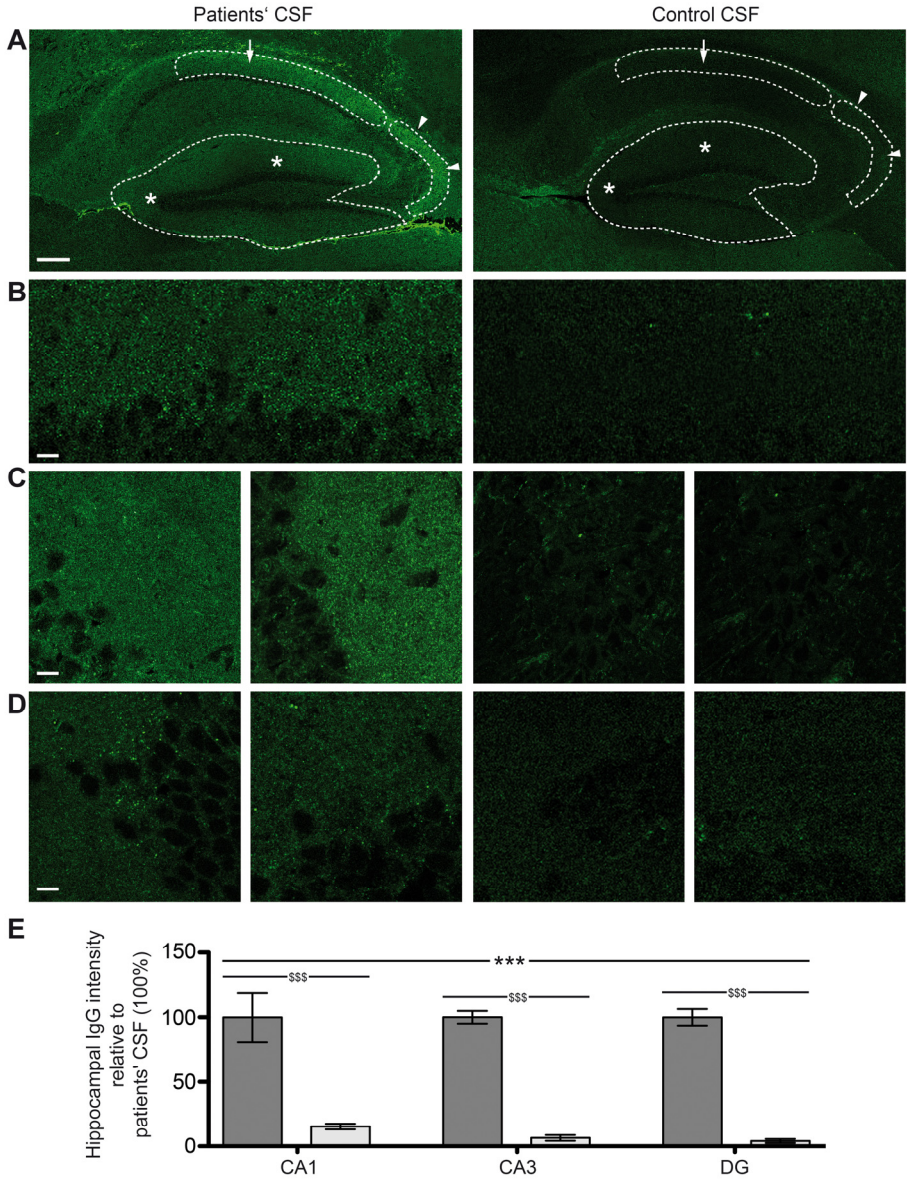

Figure 4: Confocal microscopy analysis of human IgG bound to hippocampus
Panel **A**, shows a sagittal section of the entire hippocampus with areas examined at higher magnification in **B** (arrow in CA1), **C** (arrow heads in CA3) and **D** (asterisks in dentage gyrus [DG]). The sections were obtained from animals sacrificed on day 18. Note that in the hippocampus of mice infused with patients CSF, but not with control CSF, there is a fine punctate IgG immunolabeling surrounding neuronal bodies, similar to the neuropil immunolabeling reported with indirect immunohistochemistry (e.g., tissue section directly incubated with patients' antibodies, as in (13)). Scale bar in **A**=200 µm; scale bars in **B-D**=10 µm. **(E)** Quantification of intensity of human IgG immunofluorescence in CA1, CA3, and DG (as indicated in **A**) in animals infused with patients' CSF (grey columns, n=4) or control CSF (white columns, n=3) sacrificed on day 18. Mean intensity of IgG immunostaining in the indicated area in animals treated with patients' CSF was defined as 100%. Data are presented as mean ± s.e.m. Significance of treatment effect was assessed by two-way ANOVA with an α-error of 0.05 (asterisks) and post-hoc testing with Sidak-Holm adjustment ($). ***,$$$ P<0.001. See Table 2 for detailed statistics.

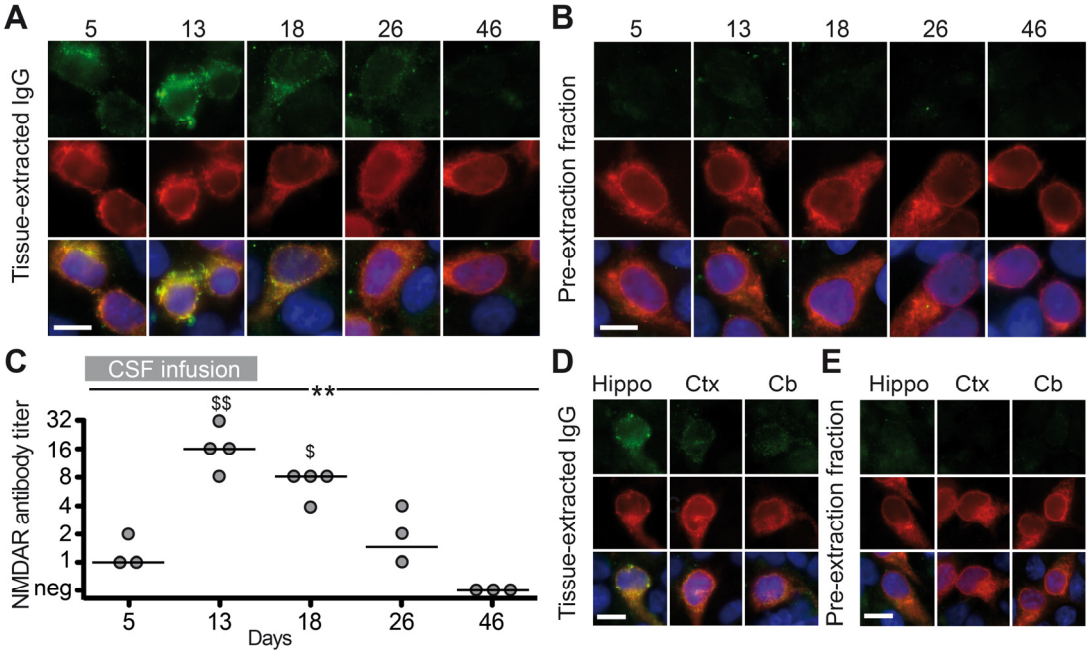

Figure 5: The human IgG extracted from brain of mice infused with patients' CSF is specific for NMDARs

(A,B) HEK293 cells expressing the GluN1 subunit of the NMDAR immunolabeled with acid-extracted IgG fractions (top row in **A**) or pre-extraction fractions (top row in **B**) from hippocampus of mice infused with patients' CSF and sacrificed on the indicated days. The maximal reactivity with GluN1-expressing cells was noted in acid-extracted IgG fractions from days 13 and 18 (**A**); none of the pre-extraction fractions showed GluN1 reactivity (**B**) indicating that the reactivity of acid-extracted fractions corresponds to IgG antibodies that were bound to brain NMDAR receptors. The second row in **A** and **B** shows the reactivity with a monoclonal GluN1 antibody, and the third row the co-localization of immunolabeling. Scale bars=10µm. **(C)** Quantification of NMDAR antibody titer in IgG-extracted fractions from hippocampus of animals treated with patients' CSF. Number of animals: day 5 n=3, day 13 n=4, day 18 n=4, day 26 n=4, and day 46 n=3. Solid line = median. Significance was tested by Kruskal-Wallis with an α-error of 0.05 (asterisks) and post-hoc testing with Dunn's test ($). *,$ $P<0.05$, **,$$ $P<0.01$. **(D, E)** HEK293 cells expressing the GluN1 subunit of the NMDAR immunolabeled with acid-extracted IgG fractions **(D)** and pre-extraction fractions **(E)** from hippocampus, cerebral cortex (Ctx) and cerebellum (Cb) of mice infused with patients' CSF (day 18). The acid-extracted IgG fraction from hippocampus showed higher level of NMDAR antibodies than those extracted from cerebral cortex (ctx) and cerebellum (Cb). Scale bars=10µm.

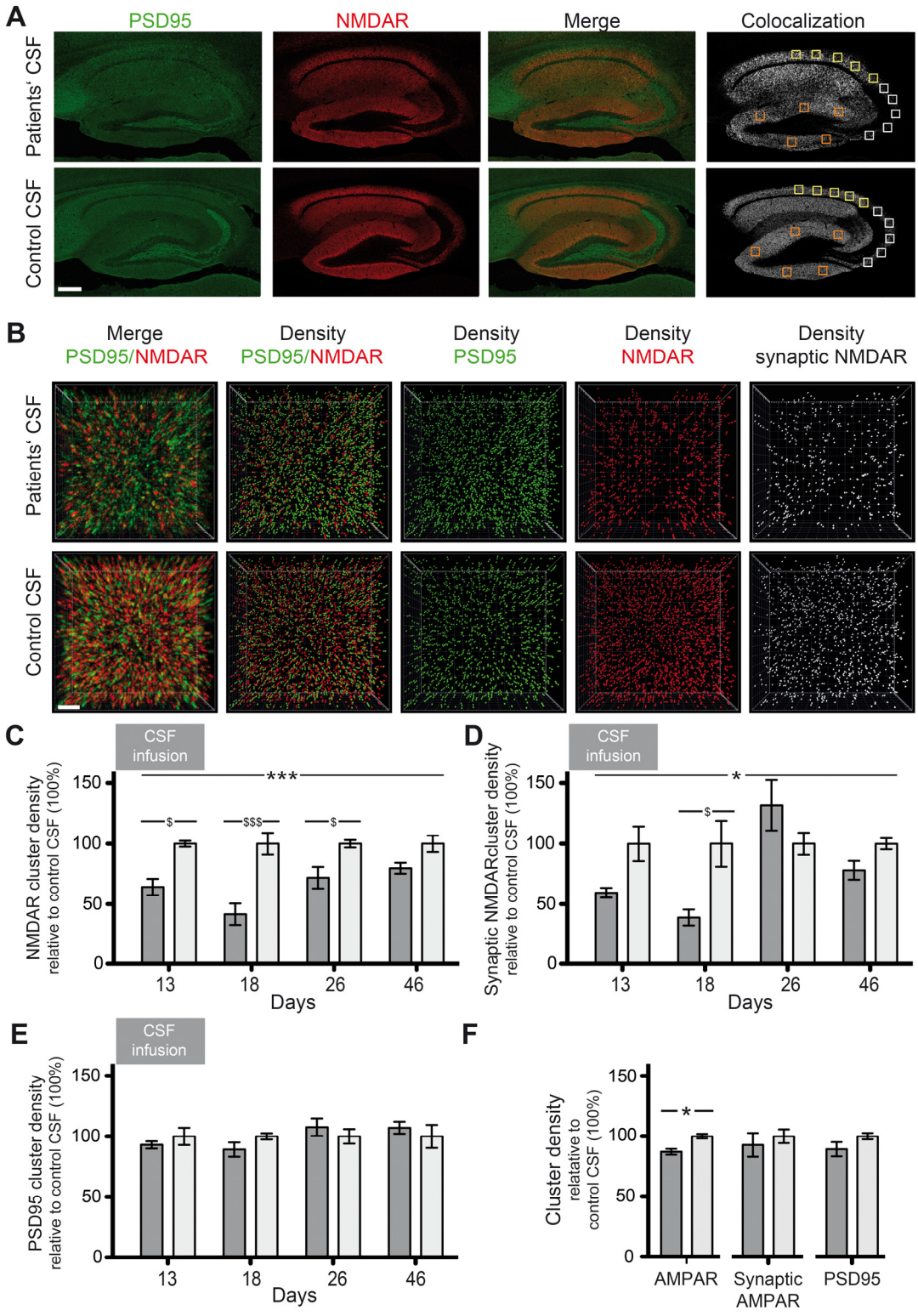

Figure 6: Patients' NMDAR antibodies selectively reduce the density of total and synaptic NMDAR clusters in hippocampus of mice

(A) Hippocampus of mice infused for 14 days (day 18) with patients' CSF (upper row) or control CSF (lower row) immunolabeled for PSD95 and NMDAR. Images were merged (merge) and post-processed to demonstrate co-localizing clusters

(colocalization). Squares in "colocalization" indicate the analyzed areas in CA1 (yellow), CA3 (white) and DG (orange). Scale bar=200 µm.
(**B**) 3D projection and analysis of the density of total clusters of PSD95 and NMDAR, and synaptic clusters of NMDAR (defined as NMDAR clusters colocalizing with PSD95) in a representative CA3 region (square in **A** "colocalization"). Merged images (merge, PSD95 green, NMDAR red) were post-processed and used to calculate the density of clusters (density=spots/μm^3). Scale bar=2 µm.
(C-F) Quantification of the density of total (**C**) and synaptic (**D**) NMDAR clusters, PSD95 clusters (**E**), and total/synaptic AMPAR clusters (**F**) in a pooled analysis of hippocampal subregions (CA1, CA3, DG) in animals treated with patients' CSF (grey) or control CSF (white) on the indicated days; AMPAR cluster density (day 18) (**F**). Mean density of clusters in control CSF treated animals was defined as 100%. Data are presented as mean ± s.e.m. Number of animals: patients' CSF day 13 n=4, day 18 n=4, day 26 n=4, day 46 n=3; control CSF day 13 n=3, day 18 n=3, day 26 n=2, day 46 n=3. Significance of treatment effect was assessed by two-way ANOVA with an α-error of 0.05 (asterisks) and post-hoc testing with Sidak-Holm adjustment ($) (C,D,E) or unpaired t-test (F). *,$$ P< 0.05; **,$$ P< 0.01; ***,$$$ P<0.001. See Table 2 for detailed statistics.

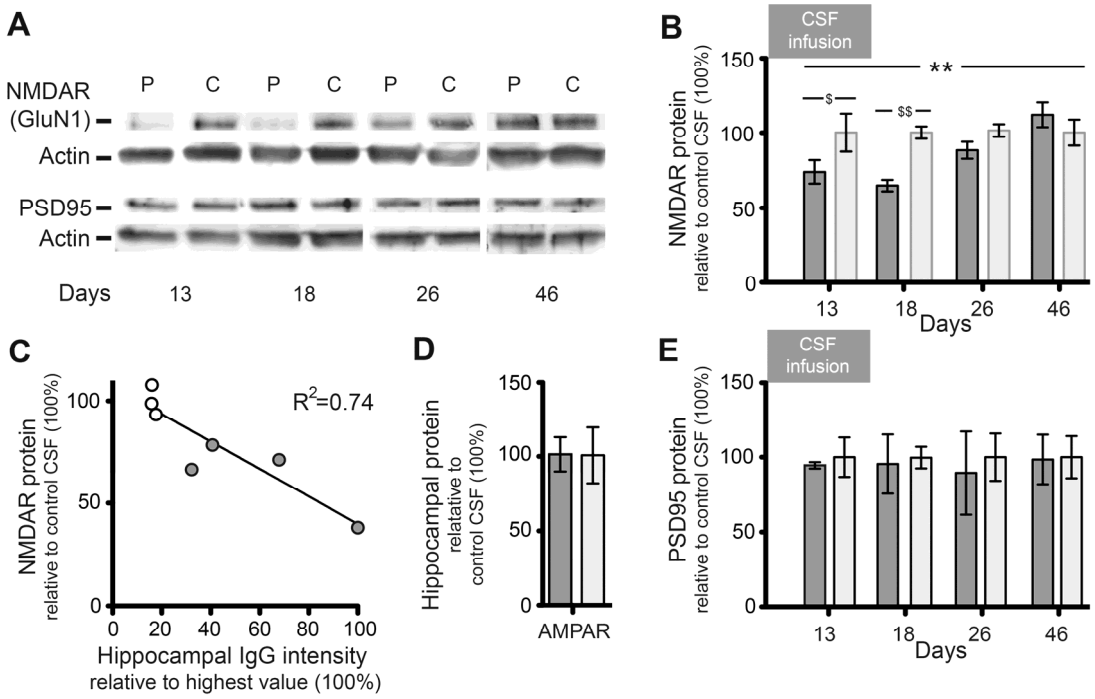

Figure 7: Patients' NMDAR antibodies selectively reduce the protein concentration of NMDAR in hippocampus of mice

A) Representative immunoblots of proteins extracted from hippocampus of animals infused with patients' CSF (P) or control CSF (C) sacrificed at the indicated time points and probed for expression of GluN1 (NMDAR), PSD95 and β-Actin (loading control). Note that there is less visible GluN1 expression on days 13 and 18.

(B, D, E) Quantification of total NMDAR **(B)**, PSD95 **(D)** or AMPAR (**E**) protein in animals treated with patients' CSF (grey columns) or control CSF (white columns) sacrificed at the indicated time points (AMPAR [**E**] day 18). Results were normalized to β-Actin (loading control). Mean band density of animals treated with control CSF was defined as 100%. Data are presented as mean ± s.e.m. Number of animals: patients' CSF day 13 n=4, day 18 n=4, day 26 n=4, day 46 n=3; control CSF day 13 n=3, day 18 n=3, day 26 n=2, day 46 n=3. Significance of treatment effect was assessed by two-way ANOVA with an α-error of 0.05 (asterisks) and post-hoc testing with Sidak-Holm adjustment ($) $ P< 0.05; **,$$ P< 0.01 See Table 2 for detailed statistics

(C) Correlation between concentration of human IgG bound to hippocampus (x-axis, highest hippocampal IgG intensity was defined as 100%) and hippocampal NMDAR protein concentration in mice sacrificed on day 18 (R^2=0.74, p=0.013). Grey circles: mice infused with patients' CSF (n=4), white circles: mice infused with control CSF (n=3).

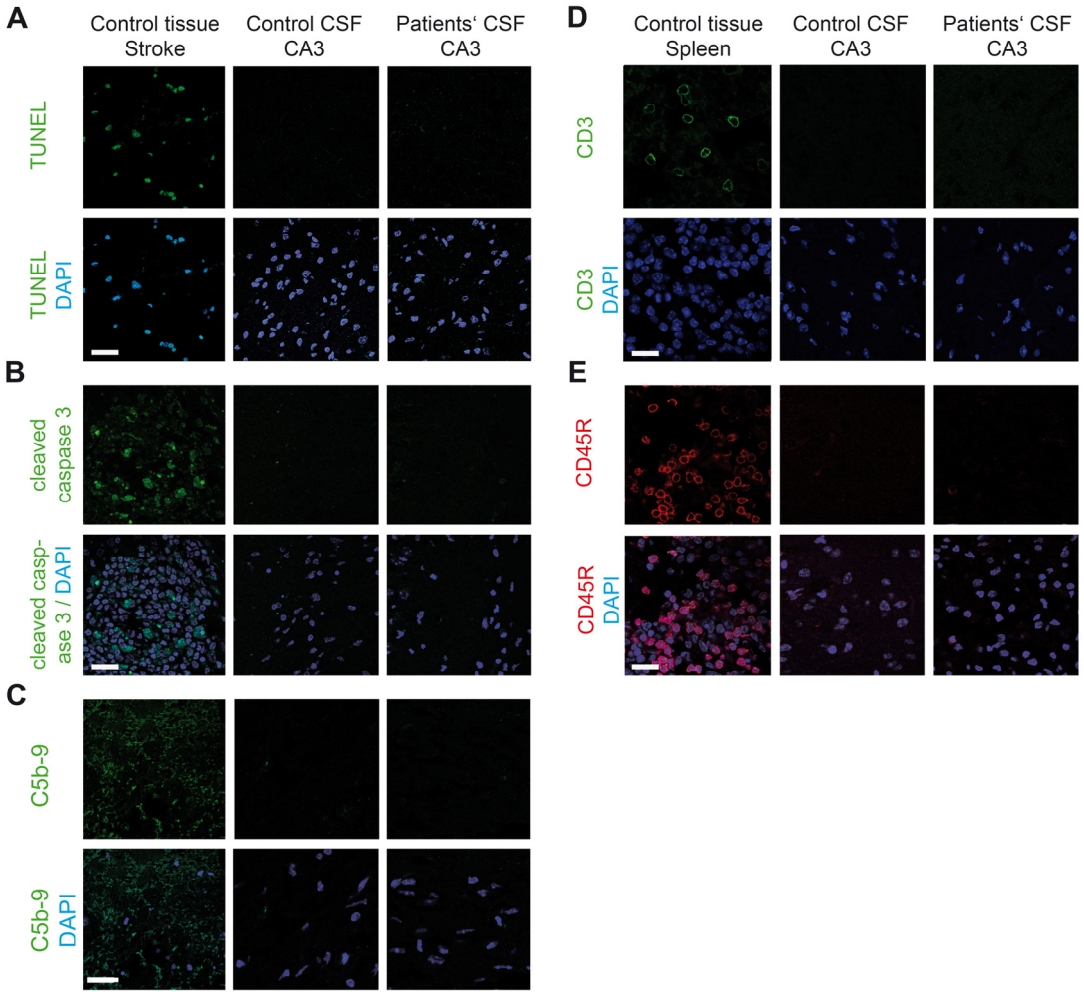

Figure 8: Absence of neuronal apoptosis, deposits of complement, and lymphocytic infiltrates in the hippocampus of mice infused with patients' CSF
(A,B) TUNEL and cleaved caspase 3 immunolabeling of a representative area of CA3 (area with maximal IgG binding and lower NMDAR concentration) of an animal infused with patients CSF, showing lack of apoptotic cells. A section of the same region in an animal with transient middle cerebral artery occlusion (stroke model) shows apoptotic cells in the penumbra (panel on the left).
(C) Same CA3 region as in (**A**) immunostained for C5b-9 showing lack of deposit of complement. A section of the same region in the indicated stroke model shows presence of complement in the penumbra (panel on the left).
(D,E) Same CA3 region as in (**A**) immunostained for T (CD3) and B (CD19) lymphocytes showing absence of inflammatory infiltrates. A section of spleen was used as control tissue showing the presence of CD3 (green) and CD19 (red) cells. Scale bar=10 µm. Total number of animals examined: patients' CSF n=4; control CSF n=3. Scale bars = 20µm

Table 1: Statistical analysis of cognitive and memory tests

		2way ANOVA analysis				Post-hoc analysis				
	Test	Variable	Source of variation	Uncorrected P-value	F-value	Day	Mean patients' CSF	Mean control CSF	Difference	Multiplicity-adjusted P-value[&]
Memory	Novel object recognition - open field	Novel object recognition index	Time	<0.001	9.96	3	0.25	0.40	-0.15	0.066
			Treatment	**<0.001**	67.5	10	0.08	0.52	-0.44	**<0.001**
			Interaction	**<0.001**	9.45	18	-0.03	0.46	-0.49	**<0.001**
						25	0.45	0.51	-0.06	0.40
		Total time of exploration (Internal control)	Time	0.003	5.48					
			Treatment	0.37	0.86					
			Interaction	0.18	1.76					
	Novel object recognition - V-maze	Novel object recognition index	Time	<0.001	12.6	3	0.35	0.41	-0.056	0.066
			Treatment	**<0.001**	24.2	10	0.15	0.46	**-0.31**	**<0.001**
			Interaction	**<0.001**	11.3	18	0.06	0.26	**-0.40**	**<0.001**
						25	0.47	0.50	-0.031	0.40
		Total time of exploration (Internal control)	Time	<0.001	14.8					
			Treatment	0.39	0.76					
			Interaction	0.37	1.07					
Anhedonia	Sucrose preference test	Percentage of sucrose preference	Time	0.30	1.22	-4 to 0	85.60	86.92	-1.33	0.89
			Treatment	0.10	2.87	10	74.64	87.66	-13.02	**0.016**
			Interaction	**0.068**	2.82	24	85.40	83.47	1.93	0.89
		Total fluid consumption (Internal control)	Time	<0.001	10.1					
			Treatment	0.50	0.46					
			Interaction	0.87	0.14					
Locomotion	Locomotor activity test	Horizontal Activity	Time	<0.001	14.6					
			Treatment	0.40	0.73					
			Interaction	0.85	0.34					
		Vertical Activity	Time	<0.001	39.0					
			Treatment	0.98	0.001					
			Interaction	0.80	0.41					
Aggressiveness	Resident-instruder test	Frequency	Time	<0.001	7.08					
			Treatment	0.16	2.04					
			Interaction	0.36	1.07					
		Latency of aggressive events	Time	0.46	0.85					
			Treatment	0.29	1.14					
			Interaction	0.98	0.068					

	Unpaired t-test / Mann Whitney-U test				
	Test, Day	Variable	mean patients' CSF (95% CI)	mean control CSF (95% CI)	Uncorrected P-value
Depression	Tail suspension test day 12	Time of immobility	169.2 (136.2-179.8)*	192.4 (165.8-208.7)*	**0,017***
	Forced swimming test day 20	Time of immobility	93.8 (72.5-115)	83.1 (58.0-108)	0.50
Anxiety	Black and white test day 6	Latency	67.8 (21.1-114)	29.2 (8.41-50.1)	0.25
		% Time in white box	12.4 (6.58-18.3)	14.9 (9.99-19.7)	0.19
		Entries in white box	6.39 (3.77-9.01)	7.00 (5.00-9.00)	0.70
		Entries in distal section	2.94 (1.46-4.43)	3.35 (2.20-4.50)	0.46
	Elevated plus maze test day 14	% Time in open arms	6.27 (2.18-10.4)	6.75 (4.12-9.38)	0.15
		Entries in open arms	5.39 (2.51-8.26)	5.80 (4.24-7.36)	0.79

In the 2-way ANOVA analysis a p-value of 0.05 is considered significant for the treatment effect. An interaction p-value < 0.10 is considered a sign of different treatment effects at different time points, warranting post-hoc analysis. Significant results are shown in bold. * Median, IQR and result of significance testing using Mann Whitney-U test indicated because of non-normality. [&] Multiplicity-adjusted P-value using Sidak-Holm post-hoc procedure.

Table 2: Statistical analysis of human IgG and receptor studies

2way ANOVA analysis					*Post-hoc analysis*				
Test	*Variable*	*Source of variation*	*P-value*	*F-value*	*Day*	*Mean patients' CSF*	*Mean control CSF*	*Differ-ence*	*Multiplicity-adjusted P-value* [&]
Immuno-histo-chemistry (Figure 3)	Human IgG intensity in percent - log transformed*	Time	0.015	3.96	3	37.1[§]	34.4[§]	-2.65	0.85
		Treatment	**<0.001**	28.2	10	60.5[§]	34.5[§]	-26.1	0.28
					18	100.0[§]	30.2[§]	-69.8	**0.012**
		Interaction	0.10	2.22	25	60.5[§]	14.7[§]	-45.8	**0.010**
					46	39.1[§]	11.0[§]	-28.1	**0.012**
Immuno-fluores-cence (Figure 4)	Human IgG intensity in percent - log transformed*	Region	0.84	0.18	CA1	100.0	4.19	95.8	**<0.001**
		Treatment	**<0.001**	121.5	CA3	100.0	6.69	93.3	**<0.001**
		Interaction	0.84	0.18	DG	100.0	15.71	84.3	**<0.001**
Confocal cluster density (Figure 6)	NMDAR - Percent of control CSF treated animals (100%)	Time	0.097	2.45	13	64.3	100.0	35.7	**0.013**
		Treatment	**<0.001**	45.5	18	41.5	100.0	58.5	**<0.001**
		Interaction	**0.097**	2.45	26	72.0	100.0	28.1	**0.026**
					46	79.8	100.0	20.2	0.081
	Synaptic NMDAR - Percent of control CSF treated animals (100%)	Time	0.016	4.48	13	59.6	100.0	40.4	0.19
		Treatment	**0.026**	5.93	18	38.8	100.0	61.2	**0.014**
		Interaction	**0.016**	4.48	26	131.8	100.0	-31.8	0.34
					46	78.1	100.0	21.9	0.72
	PSD95 - Percent of control CSF treated animals (100%)	Time	0.36	1.13					
		Treatment	0.87	0.028					
		Interaction	0.36	1.13					
Total protein - Immuno-blot (Figure 7)	NMDAR GluN1 - Percent of control CSF treated animals (100%)	Time	0.003	5.24	13	73.9	100.0	26.1	**0.019**
		Treatment	**0.008**	5.32	18	64.8	100.0	35.2	**0.002**
		Interaction	**0.009**	12.3	26	86.9	100.0	13.1	0.33
					46	111.9	100.0	-11.9	0.33
	PSD95 - Percent of control CSF treated animals (100%)	Time	0.45	0.59					
		Treatment	0.97	0.069					
		Interaction	0.97	0.070					

Kruskal-Wallis analysis				Post-hoc analysis				
Test	Variable	P-value	Test statistic	Pairwise Day	Mean rank 1	Mean rank 2	Differ-ence	P[@]
IgG extraction hippo-campus (Figure 5)	NMDAR antibody titer	**0.005**	14.7	46 vs. 5	2	5.83	-3.83	1.0
				46 vs. 13	2	15.1	-13.1	**0.002**
				46 vs. 18	2	11.8	-9.75	**0.042**
				46 vs. 26	2	7.33	-5.33	0.76

Unpaired t-test				
Test	*Variable*	*mean patients' CSF (95% CI)*	*mean control CSF (95% CI)*	*Uncorrected P-value*
Confocal cluster density (Figure 6)	AMPAR - Percent of control CSF treated animals (100%)	87.1 (76.8-97.3)	100.0 (91.8;108.2)	**0.024**
	Synaptic AMPAR - Percent of control CSF treated animals (100%)	92.8 (50.2-135.4)	100.0 (75.4;124.6)	0.57
	PSD95 - Percent of control CSF treated animals (100%)	89.1 (70.2-108.1)	100.0 (88.9-111.1)	0.17
Immuno-blot (Figure 7)	AMPAR - Percent of control CSF treated animals (100%) - day 18	100.8 (64.3-138.6)	101.4 (19.3-181.6)	0.98

In the 2-way ANOVA analysis a p-value of 0.05 is considered significant for the treatment effect. An interaction p-value < 0.10 is considered a sign of different treatment effects at different time points, warranting post-hoc analysis. Significant results are shown in bold. * 95% CI derived from log-transformed data. [&] Multiplicity-adjusted P-value using Sidak-Holm post-hoc procedure. [@] Multiplicity-adjusted P-value by Dunn's post-hoc procedure. [§] For Immunohistochemistry log transformed values were used. Mean, Difference of mean and SE of difference are derived from logarithmic values leading to skewed intervals.

Reference List

1. Lau CG, Zukin RS. NMDA receptor trafficking in synaptic plasticity and neuropsychiatric disorders. *Nat Rev Neurosci.* 2007;8(6):413-426.

2. Shepherd JD, Huganir RL. The cell biology of synaptic plasticity: AMPA receptor trafficking. *Annu Rev Cell Dev Biol.* 2007;23:613-643.

3. Mohn AR, Gainetdinov RR, Caron MG, Koller BH. Mice with reduced NMDA receptor expression display behaviors related to schizophrenia. *Cell.* 1999;98(4):427-436.

4. Belforte JE, et al. Postnatal NMDA receptor ablation in corticolimbic interneurons confers schizophrenia-like phenotypes. *Nat Neurosci.* 2010;13(1):76-83.

5. Jentsch JD, Roth RH. The neuropsychopharmacology of phencyclidine: from NMDA receptor hypofunction to the dopamine hypothesis of schizophrenia. *Neuropsychopharmacology.* 1999;20(3):201-225.

6. Mouri A, et al. Involvement of a dysfunctional dopamine-D1/N-methyl-d-aspartate-NR1 and Ca2+/calmodulin-dependent protein kinase II pathway in the impairment of latent learning in a model of schizophrenia induced by phencyclidine. *Mol Pharmacol.* 2007;71(6):1598-1609.

7. Weiner AL, Vieira L, McKay CA, Bayer MJ. Ketamine abusers presenting to the emergency department: a case series. *J Emerg Med.* 2000;18(4):447-451.

8. Gunduz-Bruce H. The acute effects of NMDA antagonism: from the rodent to the human brain. *Brain Res Rev.* 2009;60(2):279-286.

9. Hahn CG, et al. Altered neuregulin 1-erbB4 signaling contributes to NMDA receptor hypofunction in schizophrenia. *Nat Med.* 2006;12(7):824-828.

10. Snyder EM, et al. Regulation of NMDA receptor trafficking by amyloid-beta. *Nat Neurosci*. 2005;8(8):1051-1058.

11. Dalmau J, et al. Paraneoplastic anti-N-methyl-D-aspartate receptor encephalitis associated with ovarian teratoma. *Ann Neurol.* 2007;61(1):25-36.

12. Gleichman AJ, Spruce LA, Dalmau J, Seeholzer SH, Lynch DR. Anti-NMDA Receptor Encephalitis Antibody Binding Is Dependent on Amino Acid Identity of a Small Region within the GluN1 Amino Terminal Domain. *J Neurosci*. 2012;32(32):11082-11094.

13. Dalmau J, et al. Anti-NMDA-receptor encephalitis: case series and analysis of the effects of antibodies. *Lancet Neurol.* 2008;7(12):1091-1098.

14. Titulaer MJ, et al. Treatment and prognostic factors for long-term outcome in patients with anti-NMDA receptor encephalitis: an observational cohort study. *Lancet Neurol.* 2013;12(2):157-165.

15. Granerod J, et al. Causes of encephalitis and differences in their clinical presentations in England: a multicentre, population-based prospective study. *Lancet Infect Dis.* 2010;10(12):835-844.

16. Martinez-Hernandez E, Horvath J, Shiloh-Malawsky Y, Sangha N, Martinez-Lage M, Dalmau J. Analysis of complement and plasma cells in the brain of patients with anti-NMDAR encephalitis. *Neurology.* 2011;77(6):589-593.

17. Hughes EG, et al. Cellular and synaptic mechanisms of anti-NMDA receptor encephalitis. *J Neurosci* 2010;30(17):5866-5875.

18. Mikasova L, et al. Disrupted surface cross-talk between NMDA and Ephrin-B2 receptors in anti-NMDA encephalitis. *Brain.* 2012;135(Pt 5):1606-1621.

19. Bura SA, Castane A, Ledent C, Valverde O, Maldonado R. Genetic and pharmacological approaches to evaluate the interaction between the cannabinoid and cholinergic systems in cognitive processes. *Br J Pharmacol.* 2007;150(6):758-765.

20. Taglialatela G, Hogan D, Zhang WR, Dineley KT. Intermediate- and long-term recognition memory deficits in Tg2576 mice are reversed with acute calcineurin inhibition. *Behav Brain Res*. 2009;200(1):95-99.

21. Puighermanal E, Marsicano G, Busquets-Garcia A, Lutz B, Maldonado R, Ozaita A. Cannabinoid modulation of hippocampal long-term memory is mediated by mTOR signaling. *Nat Neurosci.* 2009;12(9):1152-1158.

22. Rose NR, Bona C. Defining criteria for autoimmune diseases (Witebsky's postulates revisited). *Immunol Today.* 1993;14(9):426-430.

23. Frechette ES, Zhou L, Galetta SL, Chen L, Dalmau J. Prolonged follow-up and CSF antibody titers in a patient with anti-NMDA receptor encephalitis. *Neurology.* 2011;76(7 Suppl 2):S64-S66.

24. Winters BD, Forwood SE, Cowell RA, Saksida LM, Bussey TJ. Double dissociation between the effects of peri-postrhinal cortex and hippocampal lesions on tests of object recognition and spatial memory: heterogeneity of function within the temporal lobe. *J Neurosci.* 2004;24(26):5901-5908.

25. Manto M, Dalmau J, Didelot A, Rogemond V, Honnorat J. In vivo effects of antibodies from patients with anti-NMDA receptor encephalitis: further evidence of synaptic glutamatergic dysfunction. *Orphanet J Rare Dis.* 2010;5:31.

26. Bradl M, Lassmann H. Experimental models of neuromyelitis optica. *Brain Pathol.* 2014;24(1):74-82.

27. Javitt DC, Zukin SR. Recent advances in the phencyclidine model of schizophrenia. *Am J Psychiatry.*1991;148(10):1301-1308.

28. Ferraro TN, Golden GT, Smith GG, DeMuth D, Buono RJ, Berrettini WH. Mouse strain variation in maximal electroshock seizure threshold. *Brain Res.* 2002;936(1-2):82-86.

29. Lai M, et al. AMPA receptor antibodies in limbic encephalitis alter synaptic receptor location. *Ann Neurol.* 2009;65(4):424-434.

30. Lancaster E, et al. Antibodies to the GABA(B) receptor in limbic encephalitis with seizures: case series and characterisation of the antigen. *Lancet Neurol.* 2010;9:67-76.

31. Pruss H, et al. Retrospective analysis of NMDA receptor antibodies in encephalitis of unknown origin. *Neurology.* 2010;75(19):1735-1739.

32. Gresa-Arribas N, et al. Antibody titres at diagnosis and during follow-up of anti-NMDA receptor encephalitis: a retrospective study. *Lancet Neurol.* 2014;13:167-177.

33. Aso E, et al. BDNF impairment in the hippocampus is related to enhanced despair behavior in CB1 knockout mice. *J Neurochem.* 2008;105(2):565-572.

34. Berrendero F, et al. Nicotine-induced antinociception, rewarding effects, and physical dependence are decreased in mice lacking the preproenkephalin gene. *J Neurosci.* 2005;25(5):1103-1112.

35. Bura AS, Guegan T, Zamanillo D, Vela JM, Maldonado R. Operant self-administration of a sigma ligand improves nociceptive and emotional manifestations of neuropathic pain. *Eur J Pain.* 2013;17(6):832-843.

36. Bura SA, Burokas A, Martin-Garcia E, Maldonado R. Effects of chronic nicotine on food intake and anxiety-like behaviour in CB(1) knockout mice. *Eur Neuropsychopharmacol.* 2010;20(6):369-378.

37. Burokas A, Gutierrez-Cuesta J, Martin-Garcia E, Maldonado R. Operant model of frustrated expected reward in mice. *Addict Biol.* 2012;17(4):770-782.

38. Filliol D, et al. Mice deficient for delta- and mu-opioid receptors exhibit opposing alterations of emotional responses. *Nat Genet.* 2000;25(2):195-200.

39. Llorente-Berzal A, et al. Sex-dependent psychoneuroendocrine effects of THC and MDMA in an animal model of adolescent drug consumption. *PLoS ONE.* 2013;8(11):e78386.

40. Maldonado JE, et al. Meningeal myeloma. *Arch Intern Med* 1970;126:660-663.

41. Steru L, Chermat R, Thierry B, Simon P. The tail suspension test: a new method for screening antidepressants in mice. *Psychopharmacology (Berl).* 1985;85(3):367-370.

42. Strekalova T, Gorenkova N, Schunk E, Dolgov O, Bartsch D. Selective effects of citalopram in a mouse model of stress-induced anhedonia with a control for chronic stress. *Behav Pharmacol.* 2006;17(3):271-287.

43. Caille S, Espejo EF, Reneric JP, Cador M, Koob GF, Stinus L. Total neurochemical lesion of noradrenergic neurons of the locus ceruleus does not alter either naloxone-precipitated or spontaneous opiate withdrawal nor does it influence ability of clonidine to reverse opiate withdrawal. *J Pharmacol Exp Ther.* 1999;290(2):881-892.

44. Crawley J, Goodwin FK. Preliminary report of a simple animal behavior model for the anxiolytic effects of benzodiazepines. *Pharmacol Biochem Behav.* 1980;13(2):167-170.

45. Konig M, et al. Pain responses, anxiety and aggression in mice deficient in pre-proenkephalin. *Nature*. 1996;383(6600):535-538.

46. Porsolt RD, Bertin A, Jalfre M. Behavioral despair in mice: a primary screening test for antidepressants. *Arch Int Pharmacodyn Ther*. 1977;229(2):327-336.

47. Ennaceur A. One-trial object recognition in rats and mice: methodological and theoretical issues. *Behav Brain Res.* 2010;215(2):244-254.

48. Handley SL, Mithani S. Effects of alpha-adrenoceptor agonists and antagonists in a maze-exploration model of 'fear'-motivated behaviour. *Naunyn Schmiedebergs Arch Pharmacol.* 1984;327(1):1-5.

49. Banovic D, et al. Drosophila neuroligin 1 promotes growth and postsynaptic differentiation at glutamatergic neuromuscular junctions. *Neuron.* 2010;66(5):724-738.